ACADEMIC PRESS

Available online at www.sciencedirect.com

SCIENCE DIRECT®

Journal of Sound and Vibration 261 (2003) 635–652

JOURNAL OF SOUND AND VIBRATION

www.elsevier.com/locate/jsvi

A Timoshenko-beam-on-Pasternak-foundation analogy for cylindrical shells

M. El-Mously*

Department of Civil Engineering, University of Nevada at Reno, Reno, NV 89557-0152, USA

Received 4 June 1999; accepted 7 May 2002

Abstract

A Timoshenko-beam-on-Pasternak-foundation model is developed for the analysis of thin elastic cylindrical shells. This model aims to bridge the gap between the Love–Kirchhoff theory and the approximate beam-on-elastic-foundation model of Vlasov (''long-wave'' model), which accounts for only longitudinal stretching and circumferential bending. The new model improves on the assumptions of the ''long-wave'' model by accounting for the effects of two additional actions, namely, in-plane shearing and twist. The model is used to derive ''explicit'' design formulae for (1) the fundamental natural frequencies for vibration of a uniform cylindrical shell having six sets of end restraints, and (2) the circumferential modenumbers associated with the fundamental mode. A comprehensive comparative study of the predictions of both models against available results in the literature and results obtained by the finite-element method has shown that the proposed model significantly extends the limits of the validity of the ''long-wave'' model.

1. Introduction

Cylindrical shells form key components in a wide range of industrial applications, such as aircraft, submarines, and pressure vessels. The behavior of shell structures in general, is rather complex because of the interaction between bending and stretching in carrying the applied loads. Among the early attempts to describe this interaction is that of Love [1], who derived a set of eighth-order differential equations in terms of three independent components of displacement to describe the behavior of thin shells. Despite certain shortcomings in Love's analysis, his theory proved to be sufficiently accurate for practical purposes [2]. Much effort has been made on further

*Tel.: +1-775-784-4215; fax: +1-775-784-1390.

E-mail address: mohey@scs.unr.edu (M. El-Mously).

0022-460X/03/$ - see front matter
doi:10.1016/S0022-460X(02)00995-1

refinements of Love's theory: see Leissa [3] for a comprehensive review of these theories. Koiter [2], however, showed that differences among these theories are of the same order of magnitude as the error inherent in the Love–Kirchhoff assumptions.

Closed-form solutions for the modal characteristics of cylindrical shells having their ends held circular but unrestrained axially are well known [3]. These solutions afford a valuable insight into the shell behavior and its sensitivity to changes in any of the system parameters. Corresponding expressions for other types of edge restraints are not available in the vast literature [3]. Analytical analyses have been investigated by several authors, see, Refs. [4–21].

Many attempts have been devoted to simplify Love's equations by introducing different simplifications at various stages of the formulation and/or the solution. Among the widely used theories in the literature is the Donnell–Mushtari–Vlasov (DMV) theory (also called the "shallow-shell" theory): see, Ref. [3]. This theory is based on discarding the contribution of in-plane components of deformation to the expressions for the changes of curvature of the shell middle surface; yet it leads to an eighth-order differential equation. This theory was simplified further by Vlasov [14], who assumed that the structural action of the shell is predominantly longitudinal stretching and circumferential bending, in what is referred to as the "long-wave" (LW) model. This assumption simplifies the eighth-order differential equation of the shell to a fourth-order one analogous to that of a Bernoulli–Euler beam on Winkler foundation. Yu [15] showed that the eighth-order characteristic equation of the DMV theory is considerably simplified to a fourth-order one when the circumferential wavelength of deformation is negligibly small compared to the axial one. Many authors followed the work of Vlasov [14] and Yu [15]: see, Refs. [16–20]. Though, no formal attempt has been made to quantify the limits of the validity of the LW model, Koga [20] mentioned that results obtained by the LW model are "most likely to be valid" when the shell length is about 15 or more times larger than the geometric mean of the shell radius and thickness.

The objective of this paper is two-fold: first, to present the mathematical formulation of the Timoshenko-beam-on-Pasternak-foundation (TP) model for thin elastic cylindrical shells. Second, to derive explicit design formulae for the modal characteristics of these shells. The work presented here forms part of a project illuminating the behavior of hyperboloidal cooling-tower shells, which involves some complex degenerate case effects that cannot be analyzed by the LW model. This forms the motivation for the present work.

The work begins with a brief representation of the basic equations governing the shell behavior. This is followed by a standard textbook problem in order to envisage the notion of both the LW and TP models. Next, the mathematical formulation of the TP model is presented, and a direct analogy between the shell behavior and the behavior of a TP is established. Finally, the free-vibration analysis of thin cylindrical shells having various end restraints is presented. Throughout the paper, the small-displacement theory is assumed. The material considered is assumed homogenous, linearly elastic, and isotropic.

2. Basic equations of thin cylindrical shells

Fig. 1 shows a thin-walled right circular cylindrical shell of length L, mean radius a and uniform wall thickness t defined by a right-handed orthogonal curvilinear co-ordinate system (x, θ, z)

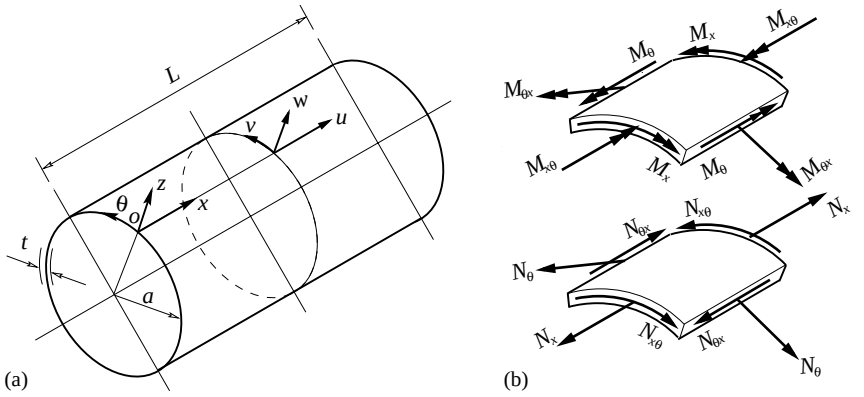

Fig. 1. (a) Cylindrical shell showing an x, θ, and z co-ordinate system and the components of small displacement in the x, θ, and z directions. (b) Small elements of the shell of (a) showing stretching- and bending-stress resultants in their positive sense. The double-headed vector notation is used to denote directions of the bending-stress resultants (right-handed rule).

where x is an axial-length co-ordinate, θ is an angular co-ordinate (in radians) and z is a radial co-ordinate (positive outwards). The shell is subjected to applied forces that vary periodically in the circumferential direction:

$$q_{xn}(x,\theta;n) = q_x(x)\cos n\theta, \quad q_{\theta n}(x,\theta;n) = q_\theta(x)\sin n\theta, \quad q_{zn}(x,\theta;n) = q_z(x)\cos n\theta, \tag{1}$$

where n is the circumferential modenumber; and q_x, q_θ, q_z are dynamic loads acting on the shell middle surface in the x, θ, and z directions, respectively (non-periodic forces can be expressed in the circumferential direction as a Fourier series). The nth-harmonic variables of the problem can be expressed as

$$\begin{aligned}&\{u_n; w_n; \varepsilon_{xn}; \varepsilon_{\theta n}; \kappa_{xn}; \kappa_{\theta n}; N_{xn}; N_{\theta n}; M_{xn}; M_{\theta n}\} = \{u; w; \varepsilon_x; \varepsilon_\theta; \kappa_x; \kappa_\theta; N_x; N_\theta; M_x; M_\theta\}\cos n\theta,\\ &\{v_n; \gamma_{x\theta n}; \tau_{x\theta n}; N_{x\theta n}; M_{x\theta n}\} = \{v; \gamma_{x\theta}; \tau_{x\theta}; N_{x\theta}; M_{x\theta}\}\sin n\theta,\end{aligned} \tag{2}$$

where u, v, and w, respectively, are the middle-surface components of displacement in the x, θ, and z directions; ε_x and ε_θ are the direct strain components in the x and θ directions; $\gamma_{x\theta}$ is the "engineering" in-plane shear strain, κ_x and κ_θ are the changes of curvature in the x and θ directions; $\tau_{x\theta}$ is the twist; N_x and N_θ are the stress resultants per unit length in the x and θ directions; $N_{x\theta}$ is the in-plane shearing-stress resultant per unit length; M_x and M_θ are the stress couples per unit length in the x and θ directions; and $M_{x\theta}$ is the twisting-stress couple per unit length.

The Lagrangian $\mathfrak{I}_{CS}$ of the vibrating shell can be written as

$$\begin{aligned}\mathfrak{I}_{CS} = &\int_L \left(\frac{C}{2}[\varepsilon_x^2 + 2\nu\varepsilon_x\varepsilon_\theta + \varepsilon_\theta^2 + (1-\nu)\gamma_{x\theta}^2/2] + \frac{D}{2}[\kappa_x^2 + 2\nu\kappa_x\kappa_\theta + \kappa_\theta^2 + 2(1-\nu)\tau_{x\theta}^2]\right)\pi a\,\mathrm{d}x\\ &- \frac{\rho t}{2}\int_L (u^{\cdot 2} + v^{\cdot 2} + w^{\cdot 2})\pi a\,\mathrm{d}x + \int_L (q_x u + q_\theta v + q_z w)\pi a\,\mathrm{d}x,\end{aligned} \tag{3}$$

where $C = Et/(1-\nu^2)$ is the shell stretching-rigidity, $D = Et^3/12(1-\nu^2)$ is the shell bending-rigidity, E is the elasticity modulus of the material; ν is Poisson's ratio; ρ is the mass density of the material; and a dot above a variable denotes differentiation with respect to time.

The three integrals on the right-hand of Eq. (3), respectively, correspond to the total elastic strain energy stored in the shell during deformation, U; the total kinetic energy acquired by the shell, T; and the work done by the applied forces, W.

The kinematics and constitutive relationships of the shell are given by

$$\varepsilon_x = u', \quad \varepsilon_\theta = \frac{nv}{a} + \frac{w}{a}, \quad \gamma_{x\theta} = v' - \frac{nu}{a}, \quad \kappa_x = -w'', \quad \kappa_\theta = \frac{n^2 w}{a^2} + \frac{nv}{a^2}, \quad \tau_{x\theta} = \frac{nw'}{a} + \frac{v'}{a}, \tag{4}$$

$$\begin{aligned} &\varepsilon_x = (N_x - \nu N_\theta)/Et, && \varepsilon_\theta = (N_\theta - \nu N_x)/Et, && \gamma_{x\theta} = N_{x\theta}/Gt, \\ &\kappa_x = 12(M_x - \nu M_\theta)/Et^3, && \kappa_\theta = 12(M_\theta - \nu M_x)/Et^3, && \tau_{x\theta} = 6M_{x\theta}/Gt^3, \end{aligned} \tag{5}$$

where a prime for a variable denotes differentiation with respect to the axial co-ordinate x, and $G = E/2(1+\nu)$ is the modulus of rigidity of the material.

3. A standard textbook problem

In order to envisage the notion of the LW model, and the proposed TP model, it is convenient to recall the static behavior of a shallow simply-supported cylindrical panel of mean radius a, axial length l and circumferential length $b = \pi a/n$, subjected to a doubly outward radial-pressure $P_o \sin(\pi x/l)\sin(n\theta)$ over the entire panel. The total strain energy, U, stored in the panel during deformation is given by

$$U = \frac{Et}{a^2}\frac{lbw_o^2}{8}\left[1 + 2(l/b)^2 + (l/b)^4\right]^{-1} + \frac{D\pi^4}{l^4}\frac{lbw_o^2}{8}[1 + 2(l/b)^2 + (l/b)^4]. \tag{6}$$

The two terms on the right-hand of Eq. (6), respectively, correspond to the stretching, U_S, and bending, U_B, components of the total strain energy U, ($U = U_S + U_B$). Note that the quadratic expression $[1 + 2(l/b)^2 + (l/b)^4]$ appears in the denominator of the stretching term, and in the numerator of the bending term. The three terms in the quadratic expression: namely, 1, $2(l/b)^2$, and $(l/b)^4$, correspond, respectively, to the contributions of ε_θ, $\gamma_{x\theta}$, and ε_x to the stretching strain energy U_S. They also correspond, respectively, to the contributions of κ_x, $\tau_{x\theta}$, and κ_θ to the bending strain energy U_B.

For large values of l/b compared with unity such that $(l/b)^4 \gg 2(l/b)^2 \gg 1$, the quadratic expression $[1 + 2(l/b)^2 + (l/b)^4]$ becomes asymptotic to $(l/b)^4$ which corresponds to the contribution of ε_x to U_S, and the contribution of κ_θ to U_B, and the LW assumptions are valid. On the other hand, when l/b is small compared with unity, such that $(l/b)^4 \ll 2(l/b)^2 \ll 1$, the quadratic expression becomes asymptotic to unity, and the strain energy expression (6) is dominated by the contributions of ε_θ and κ_x, and the shell behavior is asymptotically axisymmetric. At $l/b = 1$, the contributions of $\gamma_{x\theta}$ and $\tau_{x\theta}$ to the quadratic expression are maximum, and both the LW and axis-symmetric approximations breakdown. The proposed TP model extends the limits of the validity of the LW model by accounting for the contributions of $\gamma_{x\theta}$ and $\tau_{x\theta}$ in addition to ε_x and κ_θ of the LW model.

4. Timoshenko-beam-on-Pasternak-foundation model

It is convenient to decompose the normal component, w, of displacement into two parts: one, w_B, due to ε_x and κ_θ, and the other, w_S, due to $\gamma_{x\theta}$ and $\tau_{x\theta}$, as follows:

$$w = w_B + w_S. \tag{7}$$

Setting ε_θ and κ_x to zero, the shell constitutive and kinematics relationships simplify to

$$\varepsilon_x = N_x/C, \quad \gamma_{x\theta} = N_{xy}/Gt, \quad \kappa_\theta = M_\theta/D, \quad \tau_{x\theta} = 6M_{x\theta}/Gt^3, \tag{8}$$

$$\varepsilon_x = -\frac{aw_B''}{n^2}, \quad \gamma_{x\theta} = -\frac{w_S'}{n}, \quad \kappa_\theta = \frac{(n^2-1)w}{a^2}, \quad \tau_{x\theta} = \frac{(n^2-1)w'}{an}, \tag{9}$$

where

$$w' = w_B' + w_S' = -\frac{n^2}{a}u - n\gamma_{x\theta}. \tag{10}$$

The Lagrangian $\mathfrak{I}_{CS}$ of the vibrating shell simplifies to

$$\begin{aligned}\mathfrak{I}_{CS} = &\frac{1}{2}\int_L \left(\frac{Eta^2}{(1-\nu^2)n^4}w_B''^2 + \frac{Gt}{n^2}w_S'^2 + \frac{Et^3(n^2-1)^2}{12(1-\nu^2)a^4}w^2 + \frac{Gt^3(n^2-1)^2}{3a^2n^2}w'^2\right)\pi a\,\mathrm{d}x\\ &-\frac{1}{2}\int_L \left(\rho t(1+n^{-2})\dot{w}^2 + \frac{\rho t a^2}{n^4}\dot{w}_B'^2\right)\pi a\,\mathrm{d}x + \int_L \left(q_x u + (q_z - q_\theta/n)w\right)\pi a\,\mathrm{d}x.\end{aligned} \tag{11}$$

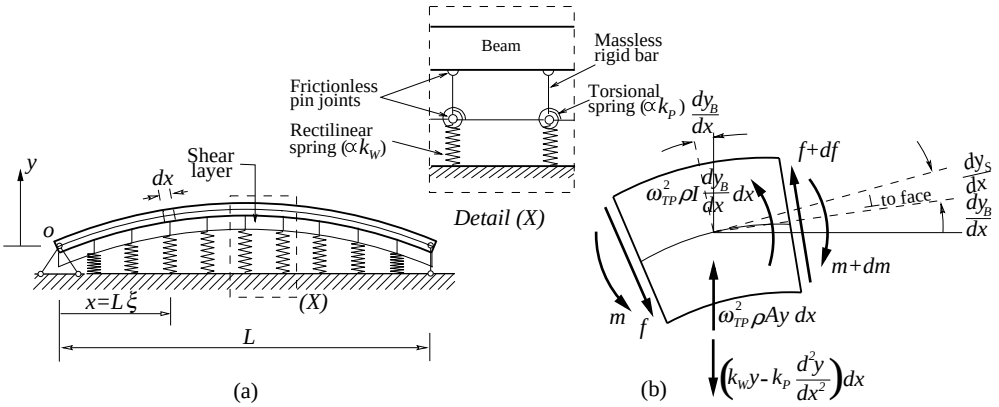

Fig. 2. (a) A freely vibrating Timoshenko beam mounted on finite Pasternak foundation. The foundation is modelled as an infinite series of massless vertical springs of stiffness k_W per unit length. The springs are connected at top by a shear layer of shearing stiffness k_P per unit length. The shear layer is modelled as a series of massless rigid bars connected by frictionless pin joints strengthened by torsion springs: see *Detail* (*X*). (b) A small element of the beam of (a) showing forces and moments acting upon the element in their positive sense.

Eq. (11) is directly analogous to the Lagrangian $\Im_{TP}$ of a finite Timoshenko beam of length L mounted on finite Pasternak foundation [22], shown in Fig. 2, given by

$$\Im_{TP} = \frac{1}{2}\int_L (EIy''^2_B + kAGy'^2_S + k_W y^2 + k_P y'^2)\,\mathrm{d}x - \frac{1}{2}\int_L (\rho A \dot{y}^2 + \rho I \dot{y}'^2_B)\,\mathrm{d}x + \int_L (p_y y + p_\psi y'_B)\,\mathrm{d}x, \tag{12}$$

where y_B and y_S are the bending and shearing components of the total lateral deflection y of the reference line; y'_B and y'_S are the slopes due to bending and shearing; ρ is the mass density of the material; E and G are the elasticity and rigidity moduli of the material, respectively; k_w and k_p are the vertical and shearing stiffnesses of the Pasternak foundation, respectively; k is a shearing-deflection coefficient; A is the area of cross-section of the beam; I is the second moment of area of cross-section around the principle axis normal to the plane of motion; and p_y and p_ψ are the lateral force and moment acting on the beam, respectively.

The compatibility equation and the constitutive relations of the beam are given by

$$y' = y'_B + y'_S, \tag{13}$$

$$m = -EIy''_B, \quad f = kAGy'_S. \tag{14}$$

5. Timoshenko-beam-on-Pasternak-foundation analogy

In Section 4, the shell and beam-foundation variables were arranged such that the axial co-ordinate x is a common co-ordinate for the beam and the shell, and that y and w are directly correlated. The quantities corresponding to the bending slope y'_B and the shearing slope y'_S of the beam are obtained from Eq. (10) and (13), as follows:

$$y'_B \Leftrightarrow -n^2 u/a, \qquad y'_S \Leftrightarrow -n\gamma_{x\theta}. \tag{15}$$

The quantities analogous to ρA, ρI, EI, kAG, are obtained by using Eqs. (11) and (12):

$$\rho A \Leftrightarrow \rho\pi at(1+n^{-2}), \quad \rho I \Leftrightarrow \rho\pi a^3 t/n^4, \quad EI \Leftrightarrow E\pi a^3 t/(1-\nu^2)n^4, \quad kAG \Leftrightarrow G\pi at/n^2. \tag{16}$$

Similarly, the quantities analogous to the Pasternak foundation variables k_W and k_P are

$$k_W \Leftrightarrow E\pi t^3(n^2-1)^2/12(1-\nu^2)a^3, \qquad k_P \Leftrightarrow G\pi t^3(n^2-1)^2/3an^2. \tag{17}$$

Finally, the quantities analogous to the applied loads, and the internal forces are given by

$$p_y \Leftrightarrow \pi a(q_z - q_\theta/n), \quad p_\psi \Leftrightarrow (\pi a^2/n^2)q_x, \quad f \Leftrightarrow -(\pi a/n)N_{x\theta}, \quad m \Leftrightarrow (\pi a^2/n^2)N_x. \tag{18}$$

6. Free vibration of cylindrical shells

The fundamental natural frequency for vibration of finite Timoshenko beams mounted on finite Pasternak foundation [22] (see Appendix A) can be expressed in the form

$$B^2_{TP} = B^2_B(1 + C_R\pi^2 R^2 + C_S\pi^2 S^2)^{-1} + B^2_W(1 + C_P\pi^2 P^2), \tag{19}$$

Table 1
Values of the constants B_B, C_S, and C_P for various sets of end restraints

	C/C	C/F	C/H	H/H	H/F	F/F
B_B	22.4	3.50	15.4	π^2	0	0
C_S	5.01	0.47	2.76	1.	0	0
C_P	1.25	0.47	1.17	1.	$3/\pi^2$	0

$$B_{TP}^2 = \frac{\rho A L^4}{EI}\omega_{TP}^2, \quad B_B^2 = \frac{\rho A L^4}{EI}\omega_B^2, \quad B_W^2 = \frac{k_W L^4}{EI}, \quad R^2 = \frac{I}{AL^2}, \quad S^2 = \frac{EI}{kAGL^2},$$
$$P^2 = \frac{k_P}{k_W L^2}, \tag{20}$$

where C_R, C_S, C_P are constants; and B_B, B_W, and B_{TP}, respectively, are non-dimensional frequency parameters for the Bernoulli–Euler beam, the Winkler foundation, and the Timoshenko beam on Pasternak foundation; R, S and P, respectively, are non-dimensional parameters quantifying the beam rotary inertia, the beam shearing flexibility, and the foundation shearing stiffness. It is worth noting that the quantity analogous to $[S^2/R^2]$ for the shell is $[2(n^2+1)/(1-\nu)]$, which is sufficiently large (for $n > 1$) to discard the effect of rotary inertia in the analogous beam. Values of B_B, C_S, and C_P, are given in Table 1 for six sets of end restraints: C/C, C/F, C/H, H/H, H/F, and F/F, where "C" stands for clamped edges; "F" stands for free edges; and "H" stands for freely supported edges describing shell edges that remain circular but not restrained axially.

By analogy, the natural frequency for vibration of a thin cylindrical shell corresponding to the lowest axial mode, is given by

$$\Omega^2 = \frac{1}{\eta_S}\left[\frac{B_B^2}{n^4\Lambda^4}\frac{1}{(1+n^{-2})}\right] + \eta_B\left[\frac{n^4}{12}\frac{(1-n^{-2})^2}{(1+n^{-2})}\right], \tag{21}$$

$$\eta_S = [1 + 2C_S(1-\nu)^{-1}(\pi a/nL)^2], \qquad \eta_B = [1 + 2C_P(1-\nu)(\pi a/nL)^2], \tag{22}$$

$$\Omega = \omega(\rho(1-\nu)^2/E)^{1/2}(a^2/t), \qquad \Lambda = Lt^{1/2}/a^{3/2}, \tag{23}$$

where Ω and Λ, respectively, are the non-dimensional frequency and the non-dimensional length of the shell; η_S and η_B, respectively, are correction factors for the LW stretching and bending components of the natural frequency Ω. For $\eta_S = \eta_B = 1$, Eq. (21) reduces to the LW expression for Ω: see, Refs. [19,20].

It is convenient for the designer to know the "fundamental" modenumber $n = n^*$ associated with the "fundamental" natural frequency $\Omega = \Omega^*$. Assuming n in Eq. (21) as a continuous variable, it can be shown that the value of $n = n^*$ that renders the natural frequency a minimum, $\Omega = \Omega^*$, is given by

$$n^* \cong \frac{\left[12^{1/8}B_B^{1/4}\Lambda^{-1/2}\right]}{\sqrt{1 + \left[\frac{3C_S}{(1-\nu)} + C_P(1-\nu)\right]\frac{\pi^2}{4(12)^{1/4}B_B^{1/2}}/\frac{\sqrt{at}}{L}}}. \tag{24}$$

The denominator of the term on the right-hand of Eq. (24) correspond to the improvements of the TP model to the predictions of the LW model (numerators). Note that H/F and F/F cylindrical shells allow for inextensional modes of deformation, for which Eq. (24) is not valid. The fundamental modenumber for those shells is $n^* = 2$.

7. Comparative study

In order to investigate the accuracy of the TP model, Eq. (21), a comprehensive comparative study has been conducted against available results in the literature, as well as results obtained by the commercial finite-element package SAP 2000. Throughout this study, the results obtained by using the SAP 2000 are based on modelling the shell using 5000 quadrilateral shell elements, with 100 elements along the circumference and 50 elements along the meridian. The large-scale computations involved in Section 7.7 of this paper, has made it necessary to develop a special purpose finite-element (FE) program which accounts for the axisymmetric nature of the shell (Appendix B). In this study, the results obtained by the developed FE program are based on modelling the shell using 100 cylindrical frusta. The discretizations used for the SAP 2000 and the developed FE programs have proven to be adequate for present purposes.

7.1. Clamped–clamped cylindrical shells

Table 2 shows a comparison between the predictions of both the LW and TP models, Eq. (21), against the experimental data collected by Koval and Cranch [16] for a C/C cylindrical shell having $L = 12\,\text{in}$, $a = 3\,\text{in}$, and $t = 0.01\,\text{in}$. The shell was made of steel having $E = 3 \times 10^7\,\text{psi}$, $\rho = 7.33 \times 10^{-4}\,\text{lb}^\text{f}\,\text{s}^2/\text{in}^4$, and $\nu = 0.3$. Table 2 also shows the predictions of the DMV theory [10], and the analytical results of the Flügge theory [24]. Also given, are the results obtained by the SAP 2000 and the developed FE programs. Table 2 shows that all theoretical predications are higher than the experimental data for Ω^*, though they successfully predict $n^* = 6$. The LW and TP predictions, respectively, for Ω^* are 6.7% and 1.2% higher than the prediction of the theory of Flügge.

Table 3 shows a comparison between the predictions of both the LW and TP models, Eq. (21), against the experimental data collected by Sewall and Naumann [11] for a C/C cylindrical shell having $L = 24\,\text{in}$, $a = 9.538\,\text{in}$, and $t = 0.0255\,\text{in}$. The shell was made of aluminum having $E = 10^7\,\text{psi}$, $\rho = 2.54 \times 10^{-4}\,\text{lb}^\text{f}\,\text{s}^2/\text{in}^4$, and $\nu = 0.315$. Table 3 also shows the analytical results of the Flügge theory [24], and the results obtained by both the SAP 2000 and the developed FE programs. All theoretical methods predict the exact value of $n^* = 8$. The predictions of both the

Table 2
Comparison of the fundamental natural frequency (cps) of a C/C cylindrical shell ($n^* = 6$) ($L = 12\,\text{in}$, $a = 3\,\text{in}$, $t = 0.01\,\text{in}$, $E = 3 \times 10^7\,\text{psi}$, $\rho = 7.33 \times 10^{-4}\,\text{lb}^\text{f}\,\text{s}^2/\text{in}^4$, $\nu = 0.3$)

Exp. [16]	DMV [10]	Flügge [24]	SAP 2000	FE (App. B)	LW Eq. (21)	TP Eq. (21)
525	552	534.77	535.12	533.2	570.54	541.36

Table 3
Comparison of the fundamental natural frequency (cps) of a C/C cylindrical shell ($n^* = 8$) ($L = 24$ in, $a = 9.538$ in, $t = 0.0255$ in, $E = 10^7$ psi, $\rho = 2.54 \times 10^{-4}$ lb^{f}s^2/in^4, $\nu = 0.315$)

Exp. [11]	Flügge [24]	SAP 2000	FE (App. B)	LW Eq. (21)	TP Eq. (21)
227	235.6363	235.8867	240.5341	254.6674	237.5570

LW and TP models, respectively, for Ω^* are 8.1% and 0.8% higher than the result of the theory of Flügge. They are also higher than the experimental data by 12.2% and 4.7%, respectively.

Table 4 shows a comparison between the predictions of both the LW and TP models, Eq. (21), against the results given by Chung [12] for three C/C cylindrical shells. The results given by Chung [12] are based on the theory of Sanders and the DMV theory (see Ref. [3]). Table 4 also shows the analytical results of the Flügge theory [24], and the results obtained by both the SAP 2000 and the developed FE programs. Table 4 shows that the predictions of the LW and TP models agree well with the results obtained from the theories of Sanders [12] and Flügge [24], except for the shortest shell ($L/(at)^{1/2} = 9$), where the predictions of the LW and TP models, respectively, for Ω^* are 4.7% lower and 28% higher than the prediction of the Sanders theory.

Table 5 shows a comparison between the predictions of both the LW and TP models, Eq. (21), against the results obtained by Lam and Loy [23] for a C/C cylindrical shell. The results of Lam and Loy [23] are based on Rayleigh–Ritz method, with the characteristic beam functions as trial modes. Table 5 also shows the analytical results of the Flügge theory [24], and the results obtained by both the SAP 2000 and the developed FE programs. Table 5 shows that the LW and TP predictions, respectively, for Ω^* are 1.7% and 0.6% higher than the result of Lam and Loy [23]. They also are 3.8% and 2.7%, respectively, higher than the result obtained from the theory of Flügge.

Table 4
Comparison of values of the fundamental frequency parameter $\Omega^* = \omega(a^2/t)(\rho(1-\nu^2)/E)^{1/2}$ and the fundamental modenumber n^* for C/C cylindrical shells having $\nu = 0.3$

L/a	a/t	n^*	Sanders [12]	DMV [12]	Flügge [24]	SAP 2000	FE (App. B)	LW	TP
10	500	4	7.5400	7.7050	7.5424	7.5519	7.521	7.9784	7.7530
10	20	2	1.1547	1.3514	1.1582	1.1519	1.1565	1.2654	1.1686
2	20	3	6.2340	6.3760	6.2404	6.1461	6.2376	7.9784[a]	5.9428

[a] This value of Ω^* corresponds to $n^* = 4$, rather than $n^* = 3$.

Table 5
Comparison of the fundamental frequency parameter $\Omega^* = \omega(a^2/t)(\rho(1-\nu^2)/E)^{1/2}$ for a C/C cylindrical shell ($n^* = 3$) having $L/a = 20$, $a/t = 500$, and $\nu = 0.3$.

Lam and Loy [23]	Flügge [24]	SAP 2000	FE (App. B)	LW Eq. (21)	TP Eq. (21)
3.6110	3.5337	3.5425	3.5466	3.6729	3.6311

Table 6
Comparison of the fundamental natural frequency (cps) of a C/F cylindrical shell ($n^* = 5$) ($L = 24.625$ in, $a = 9.538$ in, $t = 0.0255$ in, $E = 10^7$ psi, $\rho = 2.54 \times 10^{-4}$ lb^f s^2/in^4, $\nu = 0.315$)

Exp. [11]	Flügge [24]	SAP 2000	FE (App. B)	LW Eq. (21)	TP Eq. (21)
89 and 91	91.9969	92.2564	91.8391	96.0420	94.7903

Table 7
Comparison of values of the fundamental frequency parameter $\Omega^* = \omega(a^2/t)(\rho(1-\nu^2)/E)^{1/2}$ and the fundamental modenumber n^* for C/F cylindrical shells having $\nu = 0.3$

L/a	a/t	n^*	Flügge [7]	SAP 2000	FE (App. B)	LW Eq. (21)	TP Eq. (21)
10.9	100	2	1.0000	0.9970	0.9951	1.0188	1.0170
5.80	20	2	0.8944	0.8951	0.8870	0.9047	0.9099
2.62	20	2	2.0000	1.9967	1.9826	2.4181	2.0686

7.2. Clamped–free cylindrical shells

Table 6 shows a comparison between the predictions of both the LW and TP models, Eq. (21), against the experimental data collected by Sewall and Naumann [11] for a C/F cylindrical shell having $L = 24.625$ in, $a = 9.538$ in, and $t = 0.0255$ in. The shell was made of aluminum having $E = 10^7$ psi, $\rho = 2.54 \times 10^{-4}$ lb^f s^2/in^4, and $\nu = 0.315$. Table 6 also shows the analytical results of the Flügge theory [24], and the results obtained by both the SAP 2000 and the developed FE programs. All theoretical methods predict $n^* = 5$. The LW and TP predictions, respectively, for Ω^* are 6.7% and 5.3% higher than the experimental data [11]. They are also 4.4% and 3.0%, respectively, higher than the result of the theory of Flügge.

Table 7 shows a comparison between the predictions of both the LW and TP models, Eq. (21), against the results obtained by Warburton and Higgs [7] for three C/F cylindrical shells. The results of Warburton and Higgs [7] are based on the theory of Flügge. Also given in Table 7, are the results obtained by both the SAP 2000 and the developed FE programs. For the longer shells, Table 7 shows that the LW and TP predictions are in good agreement with the results of the theory of Flügge [7]. For the shortest shell ($L/(at)^{1/2} = 11.7$), the LW and TP predictions, respectively, for Ω^* are 20.9% and 3.4% higher than the prediction of the theory of Flügge [7].

7.3. Clamped–freely supported cylindrical shells

Table 8 shows a comparison between the predictions of both the LW and TP models, Eq. (21), against the results given by Sharma and Johns [18] for a clamped-ring-stiffened cylindrical shell of infinite ring stiffness. Sharma and Johns [18] used Rayleigh–Ritz method with the beam functions as trial modes, and discarded the contributions of circumferential and in-plane shearing strains to the strain energy expression of Flügge. Table 8 also shows the analytical results of the Flügge theory [24], and the results of both the SAP 2000 and the developed FE programs. Table 8 shows

Table 8
Comparison of values of the fundamental frequency parameter $\Omega^* = \omega(a^2/t)(\rho(1-\nu^2)/E)^{1/2}$ for a C/H cylindrical shell ($n^* = 2$) having $L/a = 30$, $a/t = 192$, and $\nu = 0.3$

Sharma and Johns [18]	Flügge [24]	SAP 2000	FE (App. B)	LW Eq. (21)	TP Eq. (21)
1.0729	1.0427	1.0432	1.0048	1.0682	1.0640

that the results of both the LW and TP models are in excellent agreement with the results of Sharma and Johns [18].

7.4. Freely supported–freely supported cylindrical shells

Table 9 shows a comparison between the predictions of both the LW and TP models, Eq. (21), against the experimental data collected by Sewall and Naumann [11] for an H/H cylindrical shell having $L = 24\,\text{in}$, $a = 9.538\,\text{in}$, and $t = 0.0255\,\text{in}$. The shell was made of aluminum having $E = 10^7\,\text{psi}$, $\rho = 2.54 \times 10^{-4}\,\text{lb}^f\text{s}^2/\text{in}^4$, and $\nu = 0.315$. Table 9 also shows the analytical results of the Flügge theory [24], and the results of both the SAP 2000 and the developed FE programs. All methods predict $n^* = 7$. The LW and TP predictions, respectively, for Ω^* are 1.6% and 1.0% higher than the experimental data [11].

Table 10 shows a comparison between the predictions of both the LW and TP models, Eq. (21), against the results cited by Lam and Loy [23] for three H/H cylindrical shells, using (a) the theory of Flügge, (b) the DMV theory, and (c) the three-dimensional theory of elasticity (3-D). Table 10 also shows the results obtained by both the SAP 2000 and the developed FE programs. The results of the DMV and Flügge theories for the shortest shell are based on the direct solution of the equations of motion [3,24]. Table 10 shows that the results obtained by the LW and TP models are in good agreement with the results obtained by the other methods. For the shortest shell

Table 9
Comparison of the fundamental natural frequency (cps) of a H/H cylindrical shell ($n^* = 7$) ($L = 24\,\text{in}$, $a = 9.538\,\text{in}$, $t = 0.0255\,\text{in}$, $E = 10^7\,\text{psi}$, $\rho = 2.54 \times 10^{-4}\,\text{lb}^f\text{s}^2/\text{in}^4$, $\nu = 0.315$)

Exp. [11]	Flügge [24]	SAP 2000	FE (App. B)	LW Eq. (21)	TP Eq. (21)
163 and 169	166.1947	166.2368	165.1337	168.6315	167.7026

Table 10
Comparison of values of the fundamental frequency parameter $\Omega^* = \omega(a^2/t)(\rho(1-\nu^2)/E)^{1/2}$ and the fundamental modenumber n^* of H/H cylindrical shells having $\nu = 0.3$.

L/a	a/t	n^*	DMV [23]	Flügge [23]	3-D [23]	SAP 2000	FE (App. B)	LW Eq. (21)	TP Eq. (21)
20	20	1	0.546	0.327	0.326	0.322	0.322	0.349	0.337
20	500	3	2.913	2.530	2.519	2.522	2.523	2.548	2.549
1/4	500	19	208.29[a]	208.07[a]	—	207.23	199.97	213.13[b]	196.39

[a] Obtained from the direct solution of the equations of motion [3,24].
[b] Corresponds to $n^* = 23$.

$(L/(at)^{1/2} = 5.6)$, the prediction of the TP model for Ω^* is 5.4% less than the result of the theory of Flügge, whereas the LW prediction is 2.4% higher, but with $n^* = 23$, rather than $n^* = 19$.

7.5. Freely supported–free cylindrical shells

The inextensional mode of deformation of a cylindrical shell freely supported at $x = 0$ and free at $x = L$ can be obtained (see, Ref. [19]) by setting to zero in Eq. (4) the expressions for longitudinal, circumferential, and in-plane shearing strains, given by

$$u(x,\theta) = -\frac{A}{n^2 L}\cos(n\theta), \qquad v(x,\theta) = -\frac{Ax}{nL}\sin(n\theta), \qquad w(x,\theta) = \frac{Ax}{L}\cos(n\theta), \tag{25}$$

where A is a constant, and terms in Eq. (25) corresponding to the rigid body motion are omitted. Application of the principle of conservation of energy, results in

$$\Omega^2 = \frac{n^4}{12}\frac{(1-n^{-2})^2}{(1+n^{-2})}\left[\frac{1+6(1-\nu)(a^2/n^2L^2)}{1+(3/(n^2+1))(a^2/n^2L^2)}\right]. \tag{26}$$

The denominator of the term between square brackets in Eq. (26) corresponds to the contribution of longitudinal inertia force to the kinetic energy. Discarding this term (Section 6), Eq. (26) becomes identical to Eq. (21) for H/F shells. It is interesting to note that Eq. (26) is identical to the expression given by Love [1] for the inextensional natural frequency of F/F cylindrical shells of length $2L$: see also Ref. [21].

Koga and Saito [21] used holographic interferometry to visualize the modes of deformation of an H/F shell having $L = 7.1445 \times 10^{-2}$ m, $a = 0.033$ m, and $t = 1.55 \times 10^{-4}$ m. The specimen was made of aluminum having $E = 69 \times 10^9$ N/m^2, $\rho = 3230$ kg/m^3, and $\nu = 0.3$. The fundamental natural frequency of the shell (corresponding to $n^* = 2$) according to the predictions of Eqs. (21) and (26) are 94.06 and 90.06 Hz, respectively. These results agree very well with the experimental data 94.46 Hz of Koga and Saito [21].

7.6. Free–free cylindrical shells

In the case of F/F cylindrical shells, Eq. (21) becomes identical to the expression for the inextensional frequency of F/F cylindrical shells, derived by Rayleigh (see, Refs. [3,6]). Sewall and Naumann [11] utilized an air shaker to excite an F/F cylindrical shell having $L = 25.125$ in, $a = 9.538$ in, and $t = 0.0255$ in. The shell was made of aluminum having $E = 10^7$ psi, $\rho = 2.54 \times 10^{-4}$ lb^f s^2/in^4, and $\nu = 0.315$. The fundamental frequency for the shell (corresponding to $n^* = 2$) according to Eq. (21) is 7.2243 Hz, which agree very well with the experimental data 7.2 Hz of Sewall and Naumann [11].

7.7. Comparison between the LW and TP models

Fig. 3 shows a double-logarithmic plot for $\Omega\Lambda$ against Λ of a C/C cylindrical shell having $a/t = 100$ and $\nu = 0.3$. The results obtained by the LW model (broken curves), the TP model (solid curves), and the developed FE program are all plotted for $n = 5$. Also plotted are the asymptotes of the stretching and bending contributions to the natural frequency according to the LW and TP models (light broken and light solid curves, respectively). For large values of L/a, and

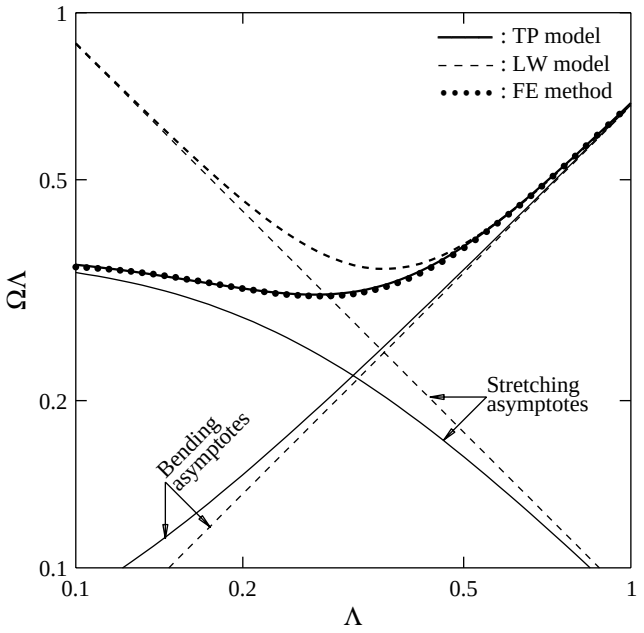

Fig. 3. A double-logarithmic plot of the non-dimensional frequency parameter $\Omega\Lambda$ against the non-dimensional length Λ of a C/C cylindrical shell with $n = 5$. Broken and solid curves, respectively, correspond to the LW and TP models, whereas dotted curves correspond to the FE results. Light curves correspond to the asymptotes of the LW and TP curves.

thus Λ, the factors η_S and η_B, Eq. (22), are asymptotic to unity, and the TP results are asymptotic to those of the LW model. On the other hand, for small values of L/a, and thus Λ, the factors η_S and η_B, Eq. (22), are increasingly significant. This reduces the stretching frequency component by an amount that depends on the value of L/a, which subsequently affects the preferred circumferential modenumber. In general, the results obtained by the TP model are in excellent agreement with the FE results, compared with those obtained by the LW model, which are only good for large values of Λ.

Fig. 4 shows a plan view of a staircase-like diagram of the circumferential modenumber n^* associated with the fundamental mode of a C/C cylindrical shell having $\nu = 0.3$. The results are plotted over a wide range of the geometric parameters L/a (0.5–20) and a/t (20–1000). The results obtained by the developed FE program are shown as alternating shaded/blank "treads". Broken and solid curves represent the boundary curves for the domains of n^* according to the LW and TP models, respectively. Lines having slope –1/2 in the logarithmic plot correspond to the dimensionless lengths $L/(at)^{1/2}$.

For large values of $L/(at)^{1/2}$, the LW results are in good agreement with the FE results. The boundary curves for the domains of n^* according to the FE are asymptotic to lines of slope $+1/2$. In this region, the shell behavior is dominated by longitudinal stretching and circumferential bending. As the value of $L/(at)^{1/2}$ decreases, the effects of in-plane shearing and twist become increasingly significant, and the LW hypothesis breaks down. On the other hand, the TP results

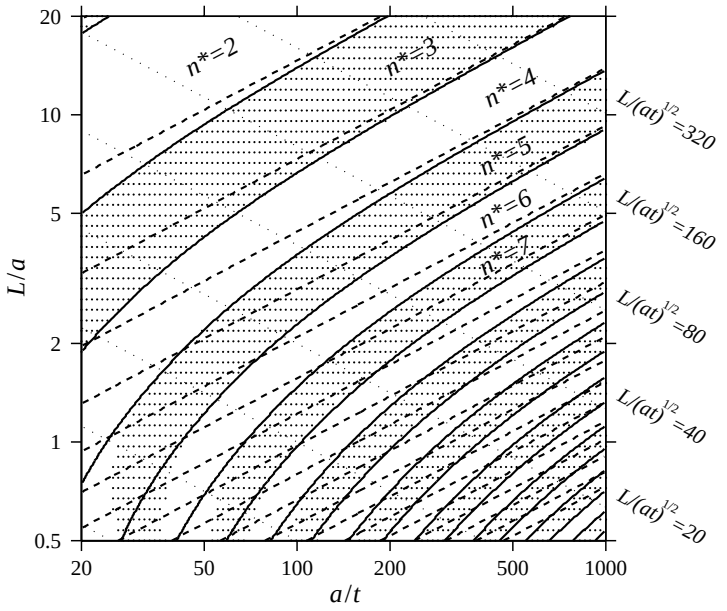

Fig. 4. A plan view of a staircase-like diagram in relation to the circumferential modenumber n^* associated with the fundamental mode of a C/C cylindrical shell ($\nu = 0.3$). The FE results are shown as alternating shaded/blank "treads". Broken and solid curves correspond, respectively, to the LW model and TP model.

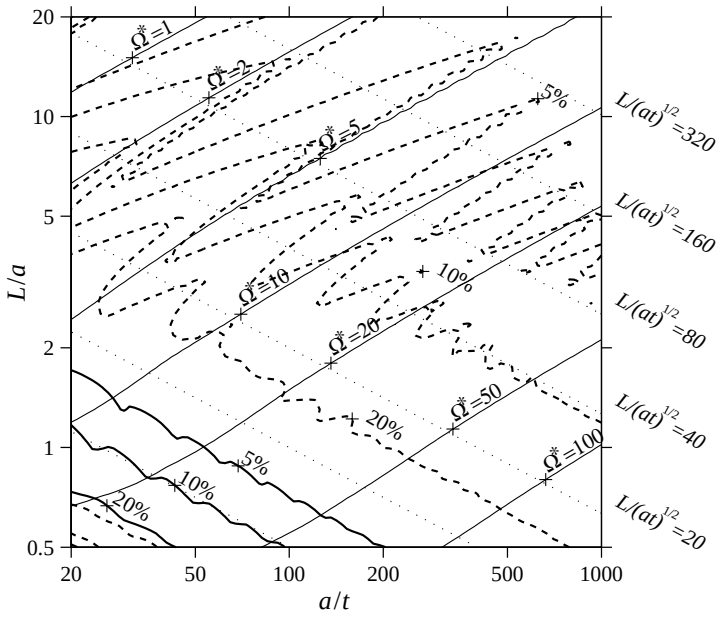

Fig. 5. Contours of the dimensionless fundamental frequency parameter Ω^* obtained by the FE method for the shell of Fig. 4. Broken and solid curves, respectively, are contours of the percentage of relative error incurred by the LW and TP models, compared with the FE results.

are in excellent agreement with the FE results except for $L/(at)^{1/2} < 5$, where the shell behavior is predominantly axisymmetric.

Fig. 5 shows contours of the dimensionless fundamental frequency parameter Ω^* obtained by the developed FE program. Also shown are contours of the percentage of relative error in Ω^* incurred by the LW model (broken curves), and the TP model (solid curves) using the FE as a standard of reference. The figure shows that contours of Ω^* are practically straight lines having a slope of $+1/2$ in the logarithmic plot. As the value of Λ increases (towards the lower right-hand corner), the value of Ω^* increases. Using the contour of 5% as a cutoff for the validity of both models, the LW model is valid for $L/(at)^{1/2} > 100$, whereas the TP model is valid for $L/(at)^{1/2} > 10$: Refs. [19, 20].

A comparative study [24] for other types of end restraints has shown that the results of the TP model for Ω^* are in excellent agreement with the FE results provided that $L/(at)^{1/2} \geqslant 8$, 6, and 2 for C/H, H/H, and C/F cylindrical shells, respectively.

8. Conclusions

On the basis of the present study, the following conclusions may be drawn:

1. A Timoshenko-beam-on-Pasternak-foundation model is developed for the analysis of thin elastic cylindrical shells. This model accounts for the effects of longitudinal stretching and circumferential bending which are considered in the "long-wave" model, in addition to the effects of in-plane shearing and twist.
2. Approximate explicit formulae are derived for (1) the fundamental natural frequency of the shell, and for (2) the circumferential modenumbers associated with the fundamental mode. A comprehensive comparative study has shown that the improved design formulae are in excellent agreement with the finite-element results provided that $L/(at)^{1/2} \geqslant 10$ for C/C and C/H cylindrical shells, and $L/(at)^{1/2} \geqslant 5$ for H/H and C/F cylindrical shells.

Acknowledgements

The author expresses his gratitude for the financial support provided by the Committee of Vice Chancellors (ORS award), UK; Cambridge Overseas Trust (KRSF Scholarship), Cambridge University, UK; and Hughes Hall (Jr. Research Fellowship), Cambridge, UK.

Appendix A. Fundamental frequencies of Timoshenko beams on Pasternak foundation (TP)

The Lagrangian $\Im_{TP}$ of a freely vibrating TP (see Eq. (12)) can be expressed as

$$\Im_{TP} = \frac{EI}{2L^3}\int_L \left(y_B''^2 + S^{-2}y_S'^2 + B_W^2 y^2 + B_W^2 P^2 y'^2\right) \mathrm{d}\xi - \frac{\rho AL}{2}\int_L \left(\dot{y}^2 + R^2\dot{y}_B'^2\right) \mathrm{d}\xi, \qquad \text{(A.1)}$$

where $R^2(= I/AL^2)$, $S^2(= EI/kAGL^2)$, and $P^2(= k_p/k_w L^2)$ are non-dimensional parameters quantifying the rotary inertia of the beam, the shearing flexibility of the beam, and the shearing stiffness of the foundation, respectively.

For $R = S = P = 0$, Eq. (A.1) reduces to that of a Bernoulli–Euler beam on Winkler foundation (BW), for which the natural frequency, ω_{BW}, can be expressed as

$$B_{BW}^2 = B_B^2 + B_W^2, \tag{A.2}$$

where $B_{BW}(= \omega_{BW} L^2(\rho A/EI)^{1/2})$ is a non-dimensional frequency parameter for the BW, $B_B(= \omega_B L^2(\rho A/EI)^{1/2})$ is a non-dimensional frequency parameter corresponding to the vibrating beam without foundation, $B_W(= (k_W L^4/EI)^{1/2})$ is a non-dimensional frequency parameter corresponding to the vibration of the beam mass on the Winkler foundation.

The effect of the beam shearing-flexibility and rotary-inertia in the Timoshenko-beam theory is to allow the beam to deform with less strain energy; thus, reducing the natural frequencies by virtue of Rayleigh's principle. Whereas the shearing stiffness of the Pasternak foundation increases the strain energy; thus, increasing the natural frequencies.

For small values of R, S, and P, the natural frequency of the TP can be expressed as

$$B_{TP}^2 \cong B_T^2 + B_P^2, \tag{A.3}$$

where $B_{TP}(= \omega_{TP} L^2(\rho A/EI)^{1/2})$ is a non-dimensional frequency parameter for the TP, $B_T(= \omega_T L^2(\rho A/EI)^{1/2})$ and $B_P(= \omega_P L^2(\rho A/EI)^{1/2})$, respectively, are non-dimensional frequency parameters corresponding to the contributions of the Timoshenko beam and the Pasternak foundation.

For a Timoshenko beam without foundation ($P = 0$), postulating the eigenmodes of the classical beam theory, y_B, as trial modes for both the bending and the shearing deflections, and application of the Lagrange's equations, results in the frequency equation

$$1 - (1 + C_R\pi^2 R^2 + C_S\pi^2 S^2)\left(\frac{B_T}{B_B}\right)^2 + (C_R\pi^2 R^2)(C_S\pi^2 S^2)\left(\frac{B_T}{B_B}\right)^4 = 0, \tag{A.4}$$

where C_R and C_S are constants depending on the type of end restraints, given by

$$C_R = \frac{1}{\pi^2}\int_0^1 y_B'^2\,\mathrm{d}\xi \Big/ \int_0^1 y_B^2\,\mathrm{d}\xi; \qquad C_S = \frac{1}{\pi^2}\int_0^1 y_B'''^2\,\mathrm{d}\xi \Big/ \int_0^1 y_B''^2\,\mathrm{d}\xi \tag{A.5, A.6}$$

and $\xi = x/L$. Discarding terms of small order of magnitude in Eq. (A.4), one finds

$$B_T \cong \frac{B_B}{\sqrt{1 + C_R\pi^2 R^2 + C_S\pi^2 S^2}}, \tag{A.7}$$

Using Rayleigh's method, the increase in B_W due to P is given by

$$B_P = B_W\sqrt{1 + C_P\pi^2 P^2}; \qquad C_P = \frac{1}{\pi^2}\int_0^1 y_B'^2\,\mathrm{d}\xi \Big/ \int_0^1 y_B^2\,\mathrm{d}\xi. \tag{A.8, A.9}$$

The fundamental natural frequency for vibration of a TP can now be expressed as

$$B_{TP}^2 = B_B^2(1 + C_R\pi^2 R^2 + C_S\pi^2 S^2)^{-1} + B_W^2(1 + C_P\pi^2 P^2). \tag{A.10}$$

A comparative study [22] has shown excellent agreement between the results of Eq. (A.10) and the "exact" solution over a wide range of practical values of R, S, and P.

Appendix B. Free-vibration analysis of cylindrical shells using the finite-element method

Following the work of Percy et al. [25], the cylindrical shell is modelled as a series of interconnected cylindrical frusta with each frustum bounded by two edge circles. The displacement field within each frustum is expressed by a Fourier series in the circumferential direction and Hermitian polynomials in the longitudinal direction. The nth harmonic components of displacement of a point on the element middle surface in the axial, u_n, tangential, v_n, and normal, w_n, directions are given by

$$u_n = [(1-\xi)u_1 + (\xi)u_2]\cos n\theta, \quad v_n = [(1-\xi)v_1 + (\xi)v_2]\sin n\theta,$$
$$w_n = [(1-3\xi^2+2\xi^3)w_1 + (\xi-2\xi^2+\xi^3)l\phi_1 + (3\xi^2-2\xi^3)w_2 + (-\xi^2+\xi^3)l\phi_2]\cos n\theta, \qquad \text{(B.1)}$$

where $(u_1, v_1, w_1, \phi_1 = (\mathrm{d}w_n/\mathrm{d}x)_1)$ and $(u_2, v_2, w_2, \phi_2 = (\mathrm{d}w_n/\mathrm{d}x)_2)$, respectively, are the amplitudes of the components of displacement and rotation at the element edge circles $x = 0$ and l (identified by subscripts 1 and 2), and l is the axial length of the frustum.

The components of the total strain energy, U_n^e, stored in the element during deformation due to stretching, U_{nS}^e, and bending, U_{nB}^e, as well as the total kinetic energy, T_n^e, acquired by the element during deformation (Eq. (3)), can be expressed as

$$U_{nS}^e = \tfrac{1}{2}\{\mathrm{q}_n^e\}^{\mathrm{T}}[\mathrm{K}_{nS}^e]\{\mathrm{q}_n^e\}; \quad U_{nB}^e = \tfrac{1}{2}\{\mathrm{q}_n^e\}^{\mathrm{T}}[\mathrm{K}_{nB}^e]\{\mathrm{q}_n^e\}; \quad T_n^e = \tfrac{1}{2}\{\dot{\mathrm{q}}_n^e\}^{\mathrm{T}}[\mathrm{K}_{nB}^e]\{\dot{\mathrm{q}}_n^e\}, \qquad \text{(B.2)}$$

where $[\mathrm{K}_{nS}^e]$ and $[\mathrm{K}_{nB}^e]$ are the element stretching and bending stiffness matrices; $[\mathrm{M}_n^e]$ is the element mass matrix; $\{\mathrm{q}_n^e\} = \{u_1, v_1, w_1, (\mathrm{d}w/\mathrm{d}x)_1, u_2, v_2, w_2, (\mathrm{d}w/\mathrm{d}x)_2\}$ is the vector of element nodal displacements and rotations; $\{\dot{\mathrm{q}}_n^e\}$ is the vector of the element nodal velocities. The three element matrices ($[\mathrm{K}_{nS}^e]$, $[\mathrm{K}_{nB}^e]$, $[\mathrm{M}_n^e]$) are derived analytically.

For a freely vibrating shell, the equations of motion of the system can be written as

$$[[\mathrm{K}_{nS}^g] + [\mathrm{K}_{nB}^g]]\{\mathrm{q}_n^g\} - \omega^2[\mathrm{M}_n^g]\{\mathrm{q}_n^g\} = \{0\}, \qquad \text{(B.3)}$$

where $[\mathrm{K}_{nS}^g]$ and $[\mathrm{K}_{nB}^g]$ are the structural stretching- and bending-stiffness matrices; $[\mathrm{M}_n^g]$ is the structural mass matrix; and $\{\mathrm{q}_n^g\}$ is the vector of nodal displacements and rotations of the structure. The solution of the eigenvalue problem, Eq. (B.3), subject to the boundary conditions, yields the natural frequencies of vibration of the shell and their corresponding mode shapes.

References

[1] A.E.H. Love, A Treatise on the Mathematical Theory of Elasticity, 4th Edition, Cambridge University Press, Cambridge, 1927.

[2] W.T. Koiter, A consistent first approximation in the general theory of thin elastic shells, Proceedings of the IUTAM Symposium on the Theory of Thin Elastic Shells, 1960, pp. 12–33.

[3] A.W. Leissa, Vibration of shells, NASA SP-228, 1973.

[4] R.N. Arnold, G.B. Warburton, Flexural vibrations of walls of thin cylindrical shells having freely supported ends, Proceedings of the Royal Society of London A 197 (1949) 238–256.

[5] K. Forsberg, Influence of boundary conditions on the modal characteristics of thin cylindrical shells, Journal of the American Institute of Aeronautics and Astronautics 2 (1964) 2150–2157.

[6] G.B. Warburton, Vibration of thin cylindrical shells, Journal of Mechanical Sciences 7 (1965) 399–407.

[7] G.B. Warburton, J. Higgs, Natural frequencies of thin cantilever cylindrical shells, Journal of Sound and Vibration 11 (1970) 335–338.

[8] C.L. Dym, Vibrations of circular cylinders, Journal of Sound and Vibration 29 (1973) 189–205.
[9] A. Ludwig, R. Krieg, An analytical quasi-exact method for calculating eigenvibrations of thin circular cylindrical shells, Journal of Sound and Vibration 74 (1981) 155–174.
[10] H. Kraus, Thin Elastic Shells, Wiley, New York, 1967.
[11] J.L. Sewall, E.C. Naumann, An experimental and analytical vibration study of thin cylindrical shells with and without longitudinal stiffeners, NASA TN D-4705, 1968.
[12] H. Chung, Free vibration analysis of circular cylindrical shells, Journal of Sound and Vibration 74 (1981) 331–350.
[13] W. Soedel, Vibrations of Plates and Shells, 2nd Edition, Marcel Dekker, New York, 1993.
[14] V.Z. Vlasov, General theory of shells and its applications in engineering, NASA TTF-99. , 1949.
[15] Y.Y. Yu, Free vibrations of thin cylindrical shells having finite lengths with freely supported and clamped edges, Journal of Applied Mechanics 22 (1955) 547–552.
[16] L.R. Koval, E.T. Cranch, On the free vibrations of thin cylindrical shells subjected to an initial static torque, Proceedings of the Fourth US National Congress of Applied Mechanics, 1962, pp. 107–117.
[17] V.I. Weingarten, Free vibration of thin cylindrical shells, Journal of the American Institute of Aeronautics and Astronautics 2 (1964) 717–722.
[18] C.B. Sharma, D.J. Johns, Vibration characteristics of a clamped-free and clamped-ring-stiffened circular cylindrical shell, Journal of Sound and Vibration 14 (1971) 459–474.
[19] C.R. Calladine, Theory of Thin Shells, Cambridge University Press, Cambridge, 1983.
[20] T. Koga, Effects of boundary conditions on the free vibrations of circular cylindrical shells, Journal of the American Institute of Aeronautics and Astronautics 26 (1988) 1387–1394.
[21] T. Koga, A. Saito, Inextensional free-vibrations of circular cylindrical shells, Journal of the American Institute of Aeronautics and Astronautics 26 (1988) 1499–1505.
[22] M. El-Mously, Fundamental frequencies of Timoshenko beams mounted on Pasternak foundation, Journal of Sound and Vibration 228 (1999) 452–457.
[23] K.Y. Lam, C.T. Loy, Effect of boundary conditions on frequencies of a multi-layered cylindrical shell, Journal of Sound and Vibration 188 (1995) 363–384.
[24] M. El-Mously, Fundamental natural frequencies of thin cylindrical shells: a comparative study, Journal of Sound and Vibration, in press.
[25] J.H. Percy, T.H.H. Pian, S. Klein, D.R. Navaratna, Application of matrix displacement method to linear elastic analysis of shells of revolution, Journal of the American Institute of Aeronautics and Astronautics 3 (1965) 2138–2145.